Modulation Processes in Power Electronic Converters

Stelios Ioannou
Electrical and Electronic Engineering, School of Sciences
University of Central Lancashire
Pyla, Larnaca, Cyprus
SIoannou2@uclan.ac.uk

Maria C. Argyrou
Electrical Engineering, Computer Engineering and Informatics
Cyprus University of Technology
Limassol, Cyprus
mx.argyrou@edu.cut.ac.cy

Mohamed Darwish
School of Engineering and Design
Brunel University
London, UK
mohamed.darwish@brunel.ac.uk

Christos C. Marouchos
Electrical Engineering, Computer Engineering and Informatics
Cyprus University of Technology
Limassol, Cyprus
christos.marouchos@cut.ac.cy

***Abstract*—This work presents an in-depth analysis and identifies the inherent modulation processes in power converters relating input and output parameters to a switching function. The timing of the switching instances and duration of the on/off periods applied to the semiconductor power switches constitutes a Switching Function. The steady state response of two popular power converters is first investigated: The AC to DC Controlled Rectifier and the PWM sinusoidally modulated 3-Level H-Bridge inverter. Both share the same power circuit configuration, namely the H-Bridge. For both configurations an appropriate switching Function acts on the input voltage to produce the output voltage in an amplitude modulation process. The same Function acts on the output current to set the input current in a similar way. The expressions relating output and input (and vice versa) with the switching function are exactly the same and easily derived from the voltage current waveforms; it is the switching function that differs. Next the mathematical models of the two converters in the time domain are derived based on the fundamental switching function expressions. The novelty here is that they are not exactly "averaging models". The switching action of the semiconductor switches is taken into account to a good degree thus giving the harmonics on output and input current. The derived models are verified using the PSIM simulation software.**

Keywords— Modulation Processes, Converters, Inverters, H-Bridge, Switching Function, Modulation Function

I. Introduction

Power Electronics date back to 1900s with the introduction of rectifiers; the mercury arc and the metal tank [1]. Their main purpose was to exploit the limitations of transformers and to convert energy at different voltages and/or frequencies [2]. However, it was not until the introduction of semiconductor switches, the thyristor followed by the Field Effect Transistor (FET) in the 1960 and 80s respectively, which revolutionized the industry of power electronics and the switched mode converters [3]-[5]. Power electronic converters fall in four categories: AC-DC, AC-AC, DC-DC and DC-AC. Using the two-port network representation, the power of converters can flow in either direction. When the power flows from the AC side towards the DC side, then the converter is said to work in the rectification-mode, whereas from DC to AC it is said that is in inverter-mode [6].

Material and manufacturing advancements keep pushing the technology offering state of the art switches with lower losses and faster switching capabilities. Gallium Nitride (GaN) offer internal resistance in the range of milli-Ohms (mΩ) and switching frequency capability as high as 200kHz [7] and 1MHz [8] which makes GaN a high performance alternative to Silicon Carbide (SiC) [9]. The range of converter applications is expanding. It is believed that 70% of today's electric energy, residential and industrial, is "converted" [1]. The list of applications includes renewables, smart grid, telecommunication, aerospace, mining, etc. The rapid growth expands the area of study, with engineers investigating new topologies and also improving the performance of existing; i.e. cascading and multi-level [10], [11]. Also, the investigation of efficiency [12] and losses [13] is of great importance for the aforementioned applications and even more important for applications involving unmanned systems which have power quality [14] restrictions and limited on-board energy availability [15]-[17].

Nowadays, the area of power electronics includes electric power, electronics and control theory. By controlling the switching of the electronic devices the output of the converters can be controlled at the desired voltage and current levels, frequency and quality (distortion and harmonics). The most efficient switching process is the Pulse Width Modulation (PWM). Modulation techniques are divided according to the switching frequency; low and high. Low switching frequency modulation includes the Selective Harmonic Elimination (SHE) and the Space Vector Control, whereas high switching frequency modulation includes Sinusoidal PWM and the Space Vector PWM. More techniques are also discussed in [18] and [19]. The main aim of these techniques is to improve the output waveforms; the amplitude of the fundamental component, the harmonic content, the effect of harmonics on the source, the switching losses and controllability.

This work presents an in-depth analysis and derives the mathematical models of the inherent modulation processes in power converters relating the input and the output parameters to a switching function. The switching action of the semiconductor switches is taken into account to a good degree thus giving also the voltage and current harmonics. The performance of the derived models is verified using the PSIM simulation software. The theoretical and simulated results are then analyzed and discussed.

II. The Common H-Bridge Configuration

Both circuits, the AC to DC Controlled rectifier and the PWM sinusoidally modulated 3-Level H-Bridge inverter shares the same power circuit configuration, namely the H-Bridge. As shown on Fig.1, the H-Bridge is composed of 4 switches and it enables load currents in both directions.

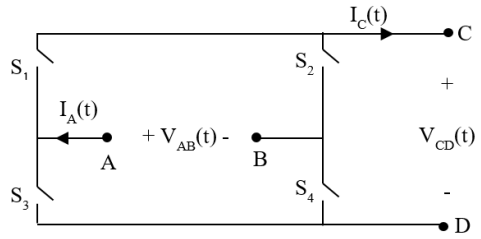

Fig. 1. H-Bridge Power Circuit Configuration

The expressions relating the output and input (and vice versa) with the switching-function *F(t)* can be derived from the input output voltages and currents as demonstrated in Fig.1. For the AC-DC controlled rectifier

$$V_{CD}(t) = F(t).V_{AB}(t) \quad (1)$$

$$I_A(t) = F(t).I_C(t) \quad (2)$$

where $V_{AB}(t)$ is the input voltage $V_{in}(t)$, $V_{CD}(t)$ is the output voltage $V_o(t)$, $I_A(t)$ is the input current $I_{in}(t)$ and $I_C(t)$ is the output current $I_o(t)$. For the inverter, the input and output are reversed

$$V_{AB}(t) = F(t).V_{CD}(t) \quad (3)$$

$$I_C(t) = F(t).I_A(t) \quad (4)$$

where $V_{AB}(t)$ is the output voltage $V_o(t)$, $V_{CD}(t)$ is the input voltage $V_{in}(t)$, $I_A(t)$ is the output current $I_{in}(t)$ and $I_C(t)$ is the input voltage $I_o(t)$.

III. The AC to DC Controlled Rectifier

The ideal switches of Fig.1 are replaced by thyristors. The Switching function of expressions (1) and (2) can easily be expressed mathematically [20] by:

$$F(t) = 4\sum_{n=1}^{\infty}\left(\frac{\sin(n\delta)}{n\pi}\cos(n\omega t - n\theta\right) \quad (5)$$

where n is an integer odd number, δ is the half ON period of the thyristors, θ is the phase delay of the Switching Function, ω is the mains frequency and α is the firing angle of the thyristors.

The input voltage is the mains (sinusoidal) voltage at frequency ω and peak (amplitude) value V_p. By applying the sum and difference trigonometric identities on expression (1) then the output voltage is derived as

$$V_o(t) = 2V_p\sum_{n=1}^{\infty}\frac{\sin(n\delta)}{n\pi}[\sin(\omega t(n+1) - \theta_n) - \sin(\omega t(n-1) - \theta_n)] \quad (6)$$

From (6) the output voltage harmonics (amplitude and phase) can be derived. Worth noting that the order of the harmonics is even since $\omega(n-1)$ where n =1,3,5..etc.

This output voltage is pushing a current through the output impedance and in most cases this current is fully smoothed to its dc value, I_{dc}. I_{dc} is easily calculated from Ohm's Law by considering the load resistance R and the average value of the output voltage. The latter is derived from (6) for n = 1. For n = 1, its second term gives rise to a term of zero frequency, hence the dc component of the output voltage.

$$V_{in}(t) = 2V_p\frac{\sin(\delta)}{\pi}\sin(\theta) \quad (7)$$

$$I_{dc} = {V_{in}}/{R} \quad (8)$$

The input current is derived from (2) and (8)

$$I_{IN}(t) = 4I_D\sum_{n=1}^{\infty}\frac{\sin(n\delta)}{n\pi}\cos(n\omega t - n\theta) \quad (9)$$

The magnitude of the input current harmonics can also be derived from (9). Worth noting that the frequency components are odd ωn, since where n =1, 3, 5...etc.

The total harmonic distortion (*THD*) for the first 50 components and displacement power factor are easily derived from (9) as expressed by (10) and (12).

$$THD = \sqrt{\sum_{n=3}^{50}\left(\frac{\frac{1}{n\pi}\sin\left(n\frac{\pi}{2}\right)}{\frac{1}{\pi}\sin\left(n\frac{\pi}{2}\right)}\right)^2} \quad (10)$$

It is evident that *THD* is independent from the value of the firing angle and level of I_{dc} for continuous conduction.

From (9) the fundamental current can be shown to be

$$I_1(t) = 4I_{dc}\frac{\sin(n\delta)}{n\pi}\sin(\omega t - \alpha) \quad (11)$$

and the displacement power factor is

$$DPF = \cos(\alpha) \quad (12)$$

IV. The PWM Sinusoidally Modulated 3-Level H-Bridge Inverter

The switching function for this circuit is a PWM signal which can be expressed in terms of a sum of switching functions [20]:

$$F_{PWMB}(t) = \sum_{k=1}^{m}\sum_{n=1}^{\infty}\frac{\sin(n\delta)}{n\pi}\cos(n\omega t - n\theta) \quad (13)$$

where m is the ratio of the switching frequency ($m\omega$) to the fundamental component (ω) of the output to be produced. k is an integer number from 1 to m, n is an integer number.

$$\delta = \frac{T}{4} + \left(\frac{D}{2}\right)\left(\frac{1}{2}\right)[\cos[(k-1)T] - \cos(kT)] \quad (14)$$

where

$$T = \frac{2\pi}{m} \quad (15)$$

$$\theta = T\left(k - \frac{1}{2}\right)n \quad (16)$$

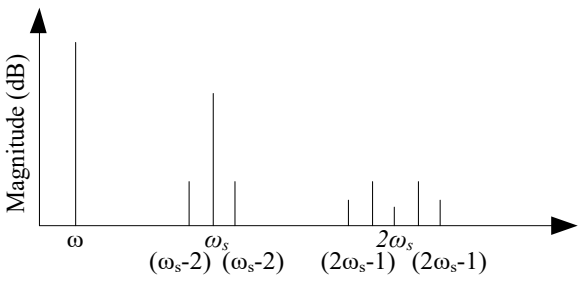

Fig. 2 Frequency Spectrum of Modulation Function

This switching function contains a strong fundamental component at ω and harmonics centred at the switching frequency $m\omega$ and its multiples, Fig. 2. Therefore the modulation function can be written in a simpler way as:

$$F_{PWMB}(t) = M_1 \sin(\omega t) + M_m \cos(m\omega t) + M_{m1} \cos[(m+2)\omega t - \theta_{m1}] + M_{m2} \cos[(m-2)\omega t - \theta_{m2}] \quad (17)$$

The output voltage is derived from (3) and (17). Certainly it will contain the same frequency components as the PWM switching as indicated in Fig.2 since the input is a dc voltage, V_{dc}.

$$V_o(t) = V_{dc}M_1 \sin(\omega t) + V_{dc}M_m \cos(m\omega t) + V_{dc}M_{m1} \cos[(m-2)\omega t - \theta_{m1}] + V_{dc}M_{m2} \cos[(m-2)\omega t - \theta_{m2}] \quad (18)$$

The output voltage at fundamental frequency $V_1(t)$ is given by

$$V_1(t) = V_{dc}M_1 sin(\omega t) \quad (19)$$

and its magnitude

$$V_1 = V_{dc}M_1 \quad (20)$$

Output current $I_o(t)$, ignoring higher order harmonics as they are smoothed by the load inductor is $I_1(t)$ is given by

$$I_1(t) = \frac{V_1}{\sqrt{R^2 + (\omega L)^2}} \sin(\omega t - \varphi) \quad (21)$$

The magnitude of the fundamental output current

$$I_1 = \frac{V_1}{\sqrt{R^2 + (\omega L)^2}} \quad (22)$$

$$\varphi = tan^{-1}\left(\frac{\omega L}{R}\right) \quad (23)$$

The output current is reflected to the input according to Expression (4)

$$I_{IN}(t) = I_o(t) F_{PWM}(t) \quad (24)$$

By substituting (17) in (24) and by employing the sum and difference trigonometric identities, the various frequency components of the input current are derived. The fundamental output current I_1 with the depth of modulation M_1 will produce the dc component of current at the input and an ac component I_{IN1} at twice the fundamental of the output current I_1, for 50Hz grid frequency it is at 100Hz.

$$I_{INdc} = \frac{I_1 M_1}{2} cos[-\varphi] \quad \text{(dc)} \quad (25)$$

$$I_{IN1} = \frac{I_1 M_1}{2} \quad \text{(100Hz)} \quad (26)$$

The fundamental output current I_1 at frequency ω (50Hz) with M_m at frequency $m\omega$ will produce at the input two components, I_{INm-1} at $(m-1)\omega$ and I_{INm+1} at $(m+1)\omega$. For a switching frequency 2000 Hz, we have at 1950Hz and I_{INm+1} at 2050Hz.

$$I_{INm-1} = \frac{I_1 M_m}{2} \quad \text{(1950Hz)} \quad (27)$$

$$I_{INm+1} = \frac{I_1 M_m}{2} \quad \text{(2050Hz)} \quad (28)$$

The fundamental output current I_1 at frequency ω (50Hz) with the component of the switching M_{m2} at frequency $(m-2)\omega$ will produce at the input two current components, I_{INm-3} at $(m-3)\omega$ and I_{INm-13} at $(m-1)\omega$. For a switching frequency 2000 Hz, we have I_{INm-3} at 1850Hz and I_{INm-13} at 1950Hz.

$$I_{INm-3} = \frac{I_1 M_{m2}}{2} \quad \text{(1850Hz)} \quad (29)$$

$$I_{INm-13} = \frac{I_1 M_{m2}}{2} \quad \text{(1950Hz)} \quad (30)$$

The fundamental output current I_1 at frequency ω (50Hz) with the component of the switching M_{m1} at frequency $(m+2)\omega$ will produce at the input two components, I_{INm+3} at $(m+3)\omega$ and I_{INm+13} $(m-1)\omega$. For a switching frequency 2000 Hz, we have I_{INm+3} at 2150Hz and I_{INm+13} at 2050Hz.

$$I_{INm+3} = \frac{I_1 M_{m1}}{2} \quad \text{(2150Hz)} \quad (31)$$

$$I_{INm+3} = \frac{I_1 M_{m1}}{2} \quad \text{(2050Hz)} \quad (32)$$

I_{INm-13} and I_{INm-1} must be added vectorially since they are at the same frequency 1950Hz. Similarly, I_{INm+1} and I_{INm+3} must be added vectorially since they are at the same frequency 2050Hz. Their phase relation cannot be derived at the moment with the present understanding of the Switching function Theory. Nevertheless the worst case scenario can be adopted and simply add them.

The current waveforms derived from a PSIM simulation are represented in Fig 3. Similarly, Fig 4 is the frequency spectrum as derived from PSIM.

This low frequency component of the input current I_{IN2} at twice the output frequency cannot be eliminated by the change of the switching frequency or the switching function. It is shown here that it is produced due to the modulation process of the output fundamental current and the modulation index itself.

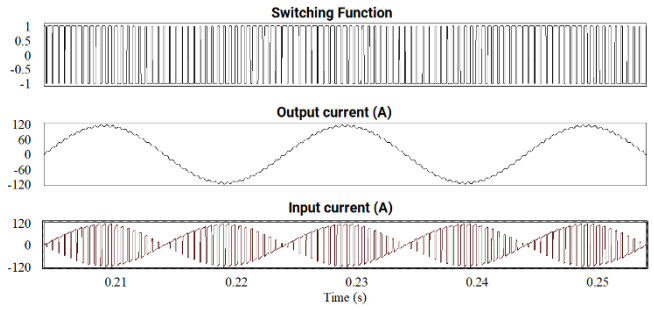

Fig.3 Switching Function, output (peak 110A) and input (peak 110A) current waveforms of the sinusoidally modulated H-Bridge 3-Level inverter

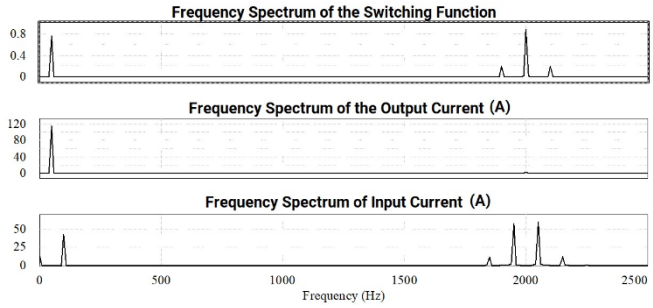

Fig.4 Frequency Spectrum of the Sinusoidally Modulated H-Bridge 3-Level Inverter

V. MATHEMATICAL MODELS

By employing the Switching Function, the large signal mathematical models of the AC to DC converter and the PWM Inverter are derived. These are suitable for simulating systems such as PV modules connected to the grid.

A. Mathematical model of the PWM Inverter

Let us consider a simple case with the inverter connected to an impedance *L*, *R*. The output voltage V_o(t) and input current i_{in}(t) are given from (33) and (34), written again as

$$V_o(t) = V_{dc}F(t) \tag{33}$$

$$i_{in}(t) = F(t)i_o\,(t) \tag{34}$$

The output loop equation is given by

$$V_o(t) = L\frac{di_o\,(t)}{dt} + \mathrm{i(t)}R \tag{35}$$

Integrating both sides of (35)

$$\int V_o(t)\mathrm{dt} = L\,i_o\,(t) + \int \mathrm{i}_o(\mathrm{t})R\ \mathrm{dt}$$

Rearranging and solving for output current, i_o(t)

$$i_o\,(t) = \frac{1}{L}\int V_o(t)\mathrm{dt} - \frac{1}{L}\int \mathrm{i}_o(\mathrm{t})R\ \mathrm{dt} \tag{36}$$

The switching function for the Inverter is given by (13) and it is approximated here to its first two components, the modulating and the switching frequency

$$F(t) = M_1\sin(\omega t) + M_m\cos(m\omega t) \tag{37}$$

The two coefficients are M_1 and M_m. M_1 is the depth of modulation and it is externally controlled. M_m is the coefficient of the switching frequency and is shown in [20] that it is related to M_1 in a fashion dictated by Fig.5.

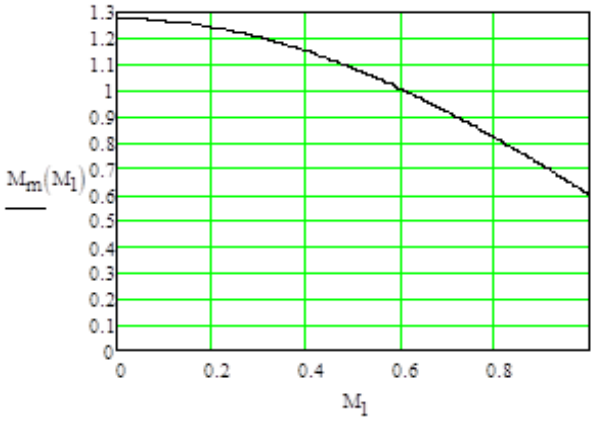

Fig.5 M_m as a function of depth of modulation M_1

The relation is not linear but it can be linearized in sections

$$\begin{aligned} M_m &= Ko - M_1K_1 && 0 < M_1 < 0.3 \\ M_m &= Ko - M_1K_{12} && 0.3 < M_1 < 0.55 \\ M_m &= Ko - M_1K_{12} && 0.055 < M_1 < 1.0 \end{aligned} \tag{38}$$

Expressions (33) to (37) are employed to construct the mathematical model of the AC to DC converter shown in Fig.6

B. Mathematical model of the AC to DC converter

Let us consider a simple case with the converter connected to an impedance *L*, *R*. The output voltage Vo(t) and input current i_{in}(t) are given from (39) and (40), written again as

$$V_o(t) = V_{in}(t)F(t) \tag{39}$$

$$i_{in}(t) = F(t)i_o\,(t) \tag{40}$$

The output loop equation is given by

$$Vo(t) = L\frac{di_o\,(t)}{dt} + \mathrm{i(t)}R \tag{41}$$

Integrating both sides of (41)

$$\int V_o(t)\mathrm{dt} = Li_o\,(t) + \int \mathrm{i}_o(\mathrm{t})R\ \mathrm{dt}$$

Rearranging and solving for output current, i_o(t)

$$i_o\,(t) = \frac{1}{L}\int V_o(t)\ \mathrm{dt} - \frac{1}{L}\int \mathrm{i}_o(\mathrm{t})R\ \mathrm{dt} \tag{42}$$

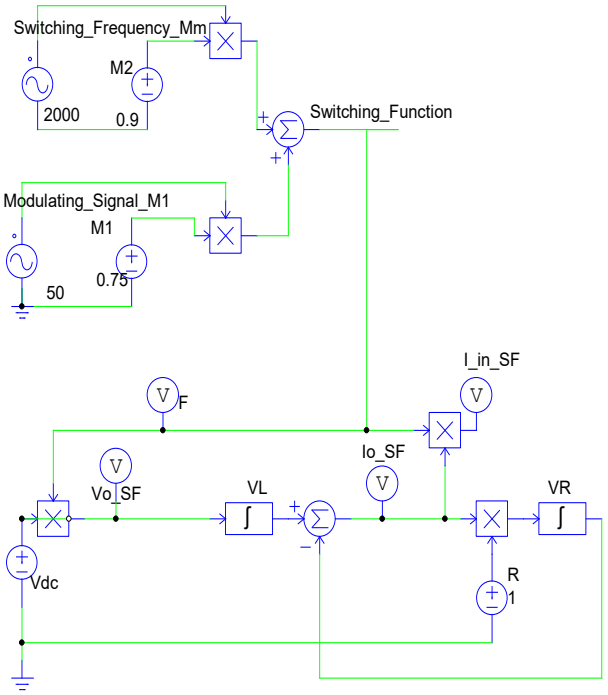

Fig.6 The Mathematical model simulated in PSIM pf the PWM inverter

The switching function for the converter is given in expression (43) and it is approximated here to its first two frequency components, the modulating and the switching frequency.

$$F(t) = K_1 \cos(\omega t - \theta) + K_3 \cos(3\omega t - 3\theta) \qquad (43)$$

The coefficients K_1 and K_3 are given by

$$K_1 = \frac{\sin(\delta)}{\pi} \text{ and } K_3 = \frac{\sin(3\delta)}{3\pi} \qquad (44)$$

$$\delta = \pi/2 \text{ and } \theta = \alpha + \delta \qquad (45)$$

where α is the firing angle and δ is the period for which the thyristors are conducting.

Expressions (39) to (45) are employed to construct the mathematical model of the AC to DC converter shown in Fig.7. The output current of the AC to DC converter is presented in Fig.8, both in PSIM simulation and in mathematical model. It is obvious that both results totally match with each other.

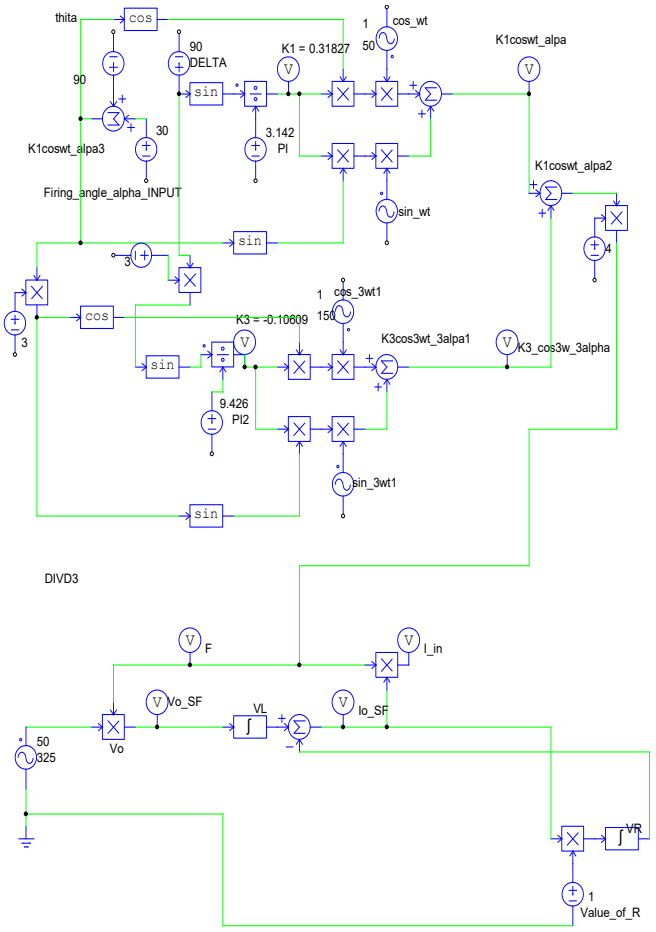

Fig.7 The mathematical model of the AC to DC converter

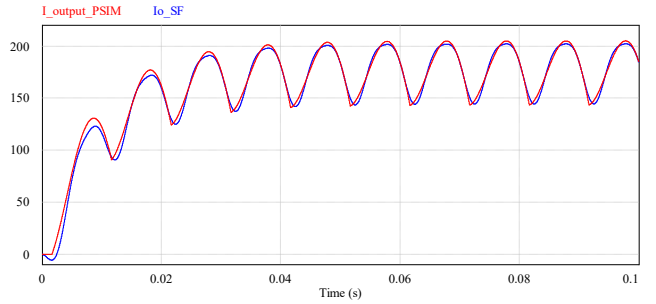

Fig.8 Output current of the AC to DC converter (Blue line is the mathematical model, red is the PSIM)

VI. Results

The results for the two circuits are presented on Tables I to IV. Table I presents the *THD,* the input current and power factor for the AC to DC converter, for both the PSIM simulation and the switching function (SF) analysis. Expression (10) is employed to calculate the *THD* whereas the fundamental current I_1 is found from (11) where δ = π/2 for continuous conduction. As shown from the tabulated results there is a good match between the PSIM simulation and the SF; the difference is limited to 1.9%.

TABLE I. AC to DC Converter L= 0.1H, R =1 Ω, α = 45°

	THD	I_1	PF
PSIM	0.464	187.6	0.700
SF	0.473	186.3	0.707

The magnitudes of the frequency components of the input currents of the PWM inverter are derived from expression (22), (25) to (30) for output of 50Hz and switching frequency of 2000Hz. As shown in Table II there is a good match between the SF results and the simulation results (PSIM). Worth noting that same frequency components, I_{INm-13} and I_{INm-1} (1950Hz) as well as I_{INm+1} and I_{INm+3} (2050Hz) are added vectorially.

TABLE II. PWM INVERTER: OUTPUT 50HZ, SWITCHING FREQUENCY 2000HZ

	I_l 50Hz	I_{dc}	I_{IN1} 100Hz	I_{INm-1} 1950Hz	I_{INm+1} 2050Hz	I_{INm-3} 1850Hz	I_{INm+3} 2150Hz
PSIM	112.7	12.95	41.98	57.18	59.47	11.27	11.45
SF	114.1	12.86	42.39	60.7	60.4	10.91	10.61

Table III presents results of the output current for the PWM inverter for L=0.01H, R=1Ω and Vdc=500V. The mathematical model based on the switching function predicts to a good accuracy the output current, both fundamental and at switching frequency.

TABLE III. INVERTER FREQUENCY COMPONENTS OF OUTPUT CURRENT

Frequency (HZ)	50	2000
From PSIM	112.7	3.477
From Math/Model SF	113.7	3.575
Error	0.89%	2.8%

Table IV presents results of the output and input current for the PWM inverter for L=0.01H, R=1Ω and Vdc=500V. The mathematical model based on the switching function predicts to a good accuracy the input current, both dc and at the lowest harmonic of 100Hz frequency.

TABLE IV. INVERTER FREQUENCY COMPONENTS OF INPUT CURRENT

Frequency (HZ)	dc	100
From PSIM	13.10	41.98
From Math/Model SF	12.95	42.63
Error	1.15%	1.55%

Table V presents results of the output current of the AC to DC Converter for L=0.1H and R=1Ω. The mathematical model based on the switching function predicts to a good accuracy the output current, both dc and at the lowest harmonic of 100Hz frequency. The second harmonic cannot be predicted as only two frequency components of the switching function are considered in the model.

TABLE V. OUTPUT CURRENT OF AC TO DC CONVERTER

Frequency	DC	100 Hz	200 Hz	300 Hz
Io Psim	179.2	28.68	4.769	1.956
Io SF	178.8	28.73	5.467	---
Error	0.22%	0.17%	14.6%	---

Table VI presents results of the input current of the AC to DC Converter for L=0.1H and R=1Ω. The mathematical model based on the switching function predicts to a good accuracy the outputτ current, both fundamental and at the first harmonic of 150Hz frequency. The second harmonic cannot be predicted as only two frequency components of the switching function are considered in the model.

TABLE VI. INPUT CURRENT OF AC TO DC CONVERTER

Frequency	50 Hz	150	250
IoPsim	239.3	60.65	36.5
Io SF	239.1	62.65	9.38
Error	0.22%	0.17%	14.6%

VII. DISCUSSION AND CONCLUSIONS

The inherent modulation processes and the existence of a modulation function in the form of the switching function in power converters are recognised and simple mathematical expressions relating input and output quantities are derived. The order of the harmonics of output voltage/current and input current are easily derived. Magnitude and phase are readily available.

The results in Table I suggest that the switching function can accurately predict currents for the AC to DC converter. In Table 2 the order and magnitudes of the input and output currents show close agreement between Switching Function predictions and PSIM simulations for the PWM Inverter.

Furthermore mathematical models suitable for simulations in more complex configurations are derived. These models take into account also the switching action of the semiconductor switches and harmonics of the output and input current are also predicted. This is a progression to the average model which is usually adopted in these cases

This paper successfully presented the potential of the switching function as a tool to give quick answers for the power converter analysis.

REFERENCES

[1] G. Zhang, B. Zhang, Z. Li,"A Brief History of Power Electronics Converters", Springer, 2018.

[2] S. Jeszenszky,"History of Transformers", IEEE Power Eng. Rev. 1996.

[3] T. G. Wilson, "The evolution of power electronics," IEEE Trans.Power Electron., vol. 15, no. 3, pp. 439–446, May 2000.

[4] B. K. Bose, "The past, present, and future of power electronics," IEEE Ind. Electron. Mag., vol. 3, no. 2, pp. 7–11, Jun. 2009.

[5] M. H. Rashid, Power Electronics Handbook: Devices Circuits and Application, 3rd ed. Burlington, MA, USA: Elsevier, 2011.

[6] I. Colak, E. Kabalci and R. Bayindir, "Review of multilevel voltage inverter topologies and control schemes," in Energy Conversion And Management 52(2011) 1114-1128, Sep. 2011.

[7] J. Xu and D. Chen, "GaN Systems - A Performance Comparison of GaN E-HEMTs Versus SiC MOSFETs in Power Switching Applications", Bodo's Power Systems 2017, Online Posting: https://gansystems.com/wp-content/uploads/2018/01/A-Performance-Comparison-of-GaN-E-HEMTs-versus-SiC-MOSFETs.pdf [19/4/19].

[8] A. Lidow, J. Strydom, A. Ferencz, and R. V. White, "Driving eGaN FETs in High Performance Power Conversion Systems", PCIM Asia, 2011.

[9] S. Davis, "Power Electronics – GaN Transistors, 2013", Online Posting:https://www.powerelectronics.com/technologies/gan-transistors/article/21863347/gan-basics-faqs [9/4/19]

[10] A. Joseph and T. R. Chelliah, "A Review of Power Electronic Converters for Variable Speed Pumped Storage Plants: Configurations, Operational Challenges, and Future Scopes", IEEE Journal of Emergingand selected topics in power electronics, 6, 1, 2018.

[11] O. H. Abdalla, H. Norallah, A. Annhwi and F. Fathi, "A Simple Staircase Modulation for A Cascaded H-bridge Multilevel Inverter", University Of Khartoum Engineering Journal, vol. 9 Issue 2 pp. 18-24, 2019.

[12] S. Ioannou, Maria C. Argyrou, CC Marouchos and M. Darwish, "Efficiency Investigation of a Grid Connected PV System with Power Smoothing", 54th International Universities Power Engineering Conference (UPEC19), Romania, 2019.

[13] S. Ioannou, CC Marouchos, M. Darwish and G. A. Putrus, “Efficiency Investigation of A Protection and Correction Solid State Device for Low-Voltage Distribution Networks”, 54th International Universities Power Engineering Conference (UPEC19), Romania, 2019.

[14] S. Ioannou, E. K. Stefanakos and P. H. Wiley, “New MOV Failure Mode Identification Invention”, IEEE Transactions on Consumer Electronics, Vol. 53, No. 3, pp.1068-1075, 2007.

[15] C. Keleshis, S. Ioannou, M. Vrekoussis, Z. Levin, M. Lange, “Data Acquisition (DAQ) System dedicated for Remote Sensing applications on Unmanned Aerial Vehicles (UAV)”, Second International Conference on Remote Sensing and Geoinformation of the Environment (RSCy2014), March 2014.

[16] G. A.Demetriou, S.Ioannou, A. Hadjipieri, I. E. Panayidou and A. Papasavva, "ERON - A PID Controlled Autonomous Surface Vessel", 18th IEEE Mediterranean Electrotechnical Conference (MELECON2016), Limassol Cyprus, 2016.

[17] S. Ioannou, K. Dalamagkidis, K. P. Valavanis, E. K. Stefanakos and P. H. Wiley, “On Improving Endurance on Unmanned Ground Vehicles: The ATRV-Jr Case Study”, 14th IEEE Mediterranean Conference on Control and Automation, June 28-30, 2006.

[18] A. Aktaibi, M. A. Rahman and A. Razali, “A Critical Review of Modulation Techniques”, 19th Annual Newfoundland Electrical and Computer Eng. Conference (NECEC 2010), IEEE, 2010.

[19] M. U.Bopche and P. V. Kapoor, “Comparative Analysis of Modulating Technique in Three Level Cascaded H-Bridge Inverter”, International Conference on Smart Electric Drives & Power System, 2018.

[20] C. C. Marouchos, "The Switching Function: analysis of power electronic circuits," in Circuits, Devices and Systems Series 17, London: Institution of Engineering and Technology, ISBN-13: 978-0863413513 ISBN-10: 0896038890.